COMMENTS ON GAS-FLUIDIZED MAGNETIZABLE BEDS IN A MAGNETIC FIELD
Part 2: Magnetization LAST mode and related phenomena

by

Jordan Y. Hristov

Review paper
UDC: 537.868:662.62–912
BIBLID: 0354–9836, *3* (1999), 1–2, 15–45

The paper continues the analysis of fluidized bed behaviour under simultaneous action of a fluidizing gas and an external magnetic field. Various problems concerning bed hydrodynamics, pressure drop, bubble control and fundamental symmetry approach are discussed with Magnetization "LAST" mode of operation.

INTRODUCTION

Basic phenomena and some introductory remarks

The behaviour of a gas-fluidized bed is determined by the balance of the forces acting upon particles: gravitational forces, fluid/particle drag forces and friction forces between particles and external fields (such as magnetic or electric) that affects fluidization [1–6]. The influence of an external field depends both on the intensity and on the orientation of the field lines [7]. The fluid flow and the magnetic field may be applied independently so those two modes already commented in the first part of the present series [8] are possible: "Magnetization FIRST" and "Magnetization LAST" mode. The latter mode involves the application of the field on preliminarily fluidized bed.

The present paper discusses some problems of gas-fluidized ferromagnetic particles with the "Magnetization LAST" mode. The main phenomena occurring under the action of an external magnetic field on free moving magnetizable particles suspended in a fluid are the particle aggregation (well known as a "magnetic flocculation") and the movement of the particles toward the zones with higher field intensity. Most of the phenomena commented here have been performed in homogeneous magnetic fields so the effects induced by the magnetic field gradients are negligible. Moreover, the fluidizing fluid considered is a gas (commonly air) so the density and viscosity effect may be

neglected too. Therefore, the main efforts of the present paper will be focused on the magnetic flocculation effects and other problems interesting for people working with gas-fluidized beds. The field effects on the pressure drop, bed expansion, bubble control as well as on the particle mobility and immobilization controllable by the field are the main discussion topics. All the materials commented exhibit normal fluidization behaviour corresponding to Geldart's group B [9].

The phenomena described allow a generalized analysis based on the phase diagrams and pseudo-thermodynamic approach employed for their design. An attempt to draw symmetry phase diagrams is done here.

It is clear from an intuitive point of view that the stronger field effects may be observed with particulate materials having higher magnetic susceptibility. The author has collected in Table 1 most of the particulate material commented here with references to their magnetic properties. The magnetization at saturation Ms is used here as a parameter presenting the magnetic properties of the particulate materials. The data in the table allow easy understanding of the phenomena commented below. All the data presented here will focus on the effect of particle material magnetic properties on the bed behaviour.

Table 1. Particle material properties commonly used in the investigations discussed

Material	Density [kg/m^3]	Ms [kA/m]	Authors employed the material & Ref.	References of material's data (Ms)
Iron	7800	1.750	Bologa and Syutkin [13] Hristov (present work)	[6, 7, 17, 18]
Magnetite	5200	478.5	Filippov [1, 9] Doichev *et al.* Hristov [6]	[6, 7, 17, 18]
Ammonia catalyst "H. Topsoe" KM-1	5100	236.4	Hristov [6]	[6, 7, 17]
Iron catalyst ICI 35/8	2700	366	Hristov [6]	[6, 7, 17, 18]
Metallurgical dross			Penchev & Hristov [17, 18] Hristov (present paper)	[7, 17, 18]
Catalyst Girdler G3L	2010	50.3	Hristov (present paper)	[17]

MAJOR EXPERIMENTAL FINDINGS

Observations and results till 1998

Most previous work on the fluidization behaviour of ferromagnetic particles in a magnetic field have been obtained by the "Magnetization FIRST" mode discussed in the first part of the series [8] . The "Magnetization LAST" mode has been an object of few independent investigations [6]. The common element of these studies is the employment axial magnetic fields (Fig.1).

Filippov [10, 11] was the first to apply the "Magnetization LAST" mode on a liquid/solid system. He called it "sedimentation" of the bed under the influence of a magnetic field. The gross bed behaviour is that due to the induced interparticle forces the fluidized particles (Fig. 1 in [8]) aggregate. The bed collapses with the increase of the field intensity down to a fixed bed state termed by Filippov a "pseudopolymeric" bed.

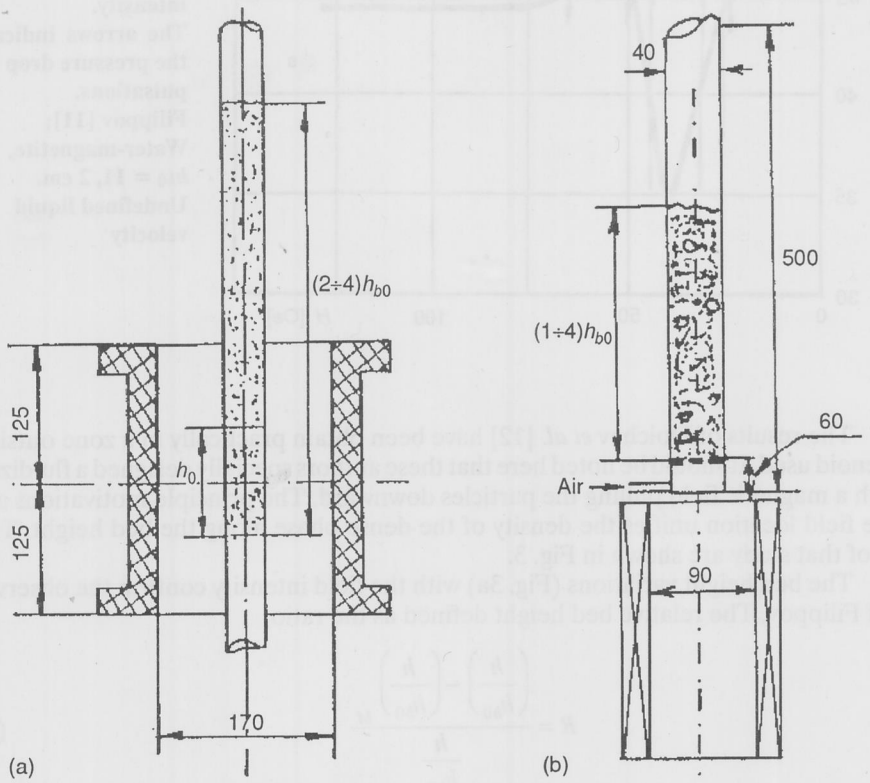

Figure 1. Experimental situations used

(a) Filippov [10, 11]; (b) Doichev et al. [12]. Dimensions in millimeters

Unfortunately data concerning details of the magnetic systems used are not available in the works of Zrunchev and Popova [14, 15] and Bologa and Syutkin [13]

The same approach has been employed also by Doichev *et al.* [12] in hydrodynamic studies on enhanced separations of magnetite sands. The data published by Bologa and Syutkin [13] confirm the same gross bed behaviour.

Figure 1 shows that the experimental set-ups used are quite different. Because of that the results obtained should be analyzed with caution taking into account the condition imposed by the magnetic field. Filippov's experimental data, illustrating the relationship between pressure drop and field intensity is shown in Fig. 2. According to this author, the curve has a characteristic shape with a minimum (the arrows indicate the pressure pulsations due to fluidization instability [10, 11]).

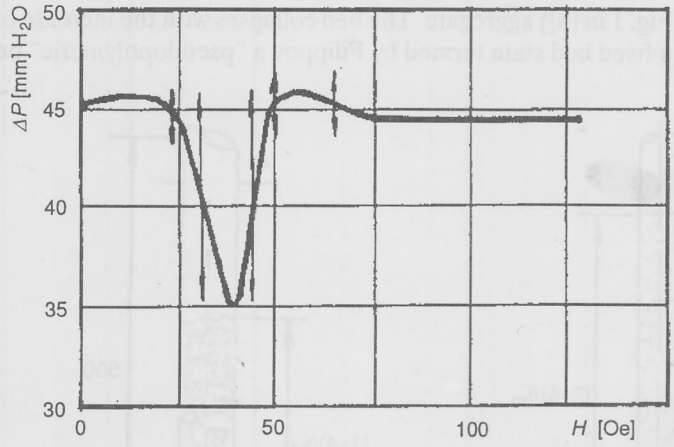

Figure 2. Pressure drop as a function of the magnetic field intensity. The arrows indicate the pressure drop pulsations. Filippov [11]; Water-magnetite, h_{b0} = 11, 2 cm. Undefined liquid velocity

The results of Doichev *et al.* [12] have been obtain practically in a zone outside the solenoid used. It should be noted here that these authors specially designed a fluidized bed with a magnetic field pulling the particles downward. The principle motivations are that the field location unifies the density of the dense phase along the bed height. The results of that study are shown in Fig. 3.

The bed height variations (Fig. 3a) with the field intensity confirm the observations of Filippov. The relative bed height defined as the ratio

$$R = \frac{\left(\frac{h}{h_{b0}}\right) - \left(\frac{h}{h_{b0}}\right)_M}{\frac{h}{h_{b0}}} \tag{1}$$

is shown in Fig. 3b. The authors pointed out that the curves have maxima. Moreover, R increases with the increase of h/h_{b0} in the range of $h/h_{b0}<3\div3.5$. The further bed expansion leads to opposite results. The explanation given in [12] is quite complicated and unclear. These results will be commented further from the viewpoint of the recent

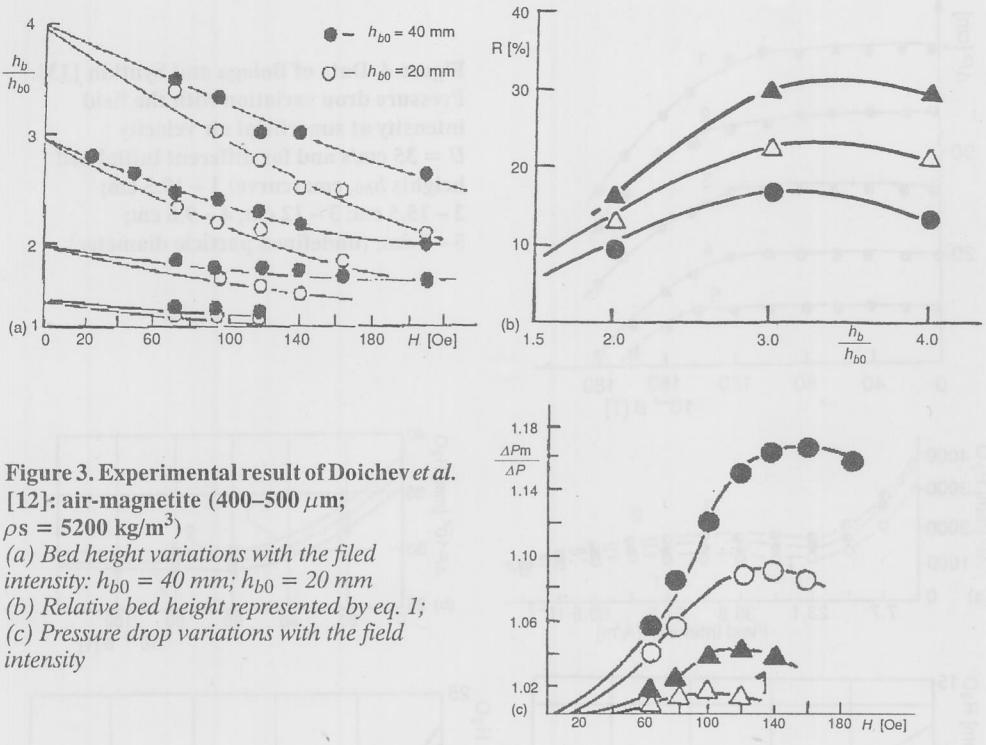

Figure 3. Experimental result of Doichev *et al.* [12]: air-magnetite (400–500 μm; ρs = 5200 kg/m^3)
(a) Bed height variations with the filed intensity: h_{b0} = 40 mm; h_{b0} = 20 mm
(b) Relative bed height represented by eq. 1;
(c) Pressure drop variations with the field intensity

finding [6]. The pressure drop data are plotted in Fig. 3c. The curves have maxima that do not confirm the curve of Filippov (Fig. 2). These curves will be analyzed further.

Bologa and Syutkin [13] claim that with the increase of magnetic field intensity the bed depth increases, but at the same time pressure drop decreases above certain field intensity (Fig. 4). These results have no explanation and they will be commented further in order to elucidate the reasons for them. Bologa and Syutkin did not describe the magnetic system used. In accordance with the text of their paper a solenoid generating an axial field is used.

Zrunchev and Popova [14] reported a bed collapse curve shown in Fig. 5. Unfortunately the data concerning the experimental conditions are not complete [14–16]. Their claim (like Bologa and Syutkin) that a solenoid generates the field applied.

Recent results

Experimental conditions required and major experimental data

The recent experiments [6] have been performed in homogeneous magnetic fields with two orientations: axial and transverse. The experimental set-ups are shown schematically in Fig. 6 and technical details are available elsewhere [6, 17, 18]. The

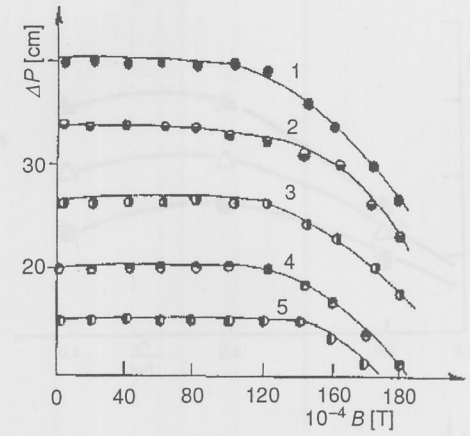

Figure 4. Data of Bologa and Syutkin [13]. Pressure drop variation with the field intensity at superficial air velocity U = 35 cm/s and for different initial bed heights h_{b0}, cm: (curve) 1 – 19.5 cm; 2 – 15.5 cm; 3 – 12 cm; 4 – 9.6 cm; 5 – 7 cm; (undefined particle diameter)

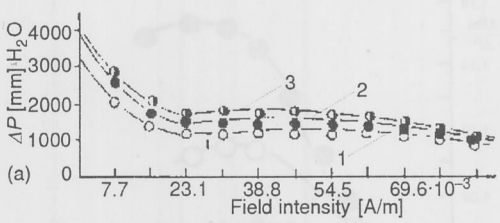

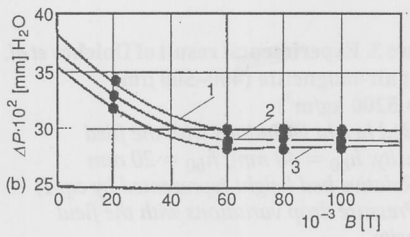

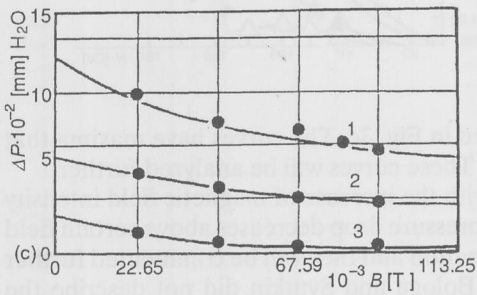

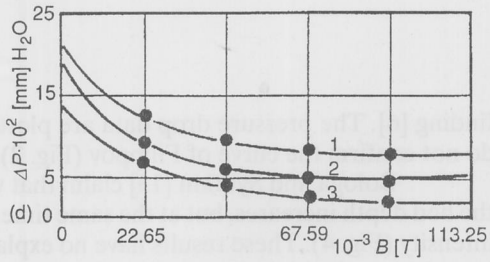

Figure 5. Pressure drop decrease with the increase of the field intensity (Zrunchev and Popova) under various experimental conditions. Undefined magnetite ammonia catalyst – air

(a) [14] d_p = 1.1 mm; U = 0.7 m/s; Effect of the temperature. Line: 1 – 400 °C; 2 – 500 °C; 3 – 550 °C;

(b) [15] d_p = 0.9 mm; U = 1 m/s. Effect of the temperature. Line: 1 – 400 °C; 2 – 500 °C; 3 – 600 °C;

(c) [15] d_p = 1.5 mm; U = 0.56 m/s; Dc = 80 mm. Effect of the ratio h_{b0}/Dc. Line: 1 – h_{b0}/Dc = 12.5; 2 – h_{b0}/Dc = 5; 3 – h_{b0}/Dc = 1

(d) [15], d_p = 1.5 mm; U = 0.9 m/s. Effect of the column diameter Dc. Line: 1 – Dc = 20 mm;

heterogeneity of the axial field (generated by a Helmholtz pair) did not exceed 1% in cylinder with dimensions 200 mm × 100 mm [17]. In the case of saddle coils used the heterogeneity did not exceed 1 % in the radial direction and 1.5 % in the axial direction for cylinder 300 mm in height and 150 mm in diameter [18]. These details will be used further for better understanding the effect of the experimental conditions on the results.

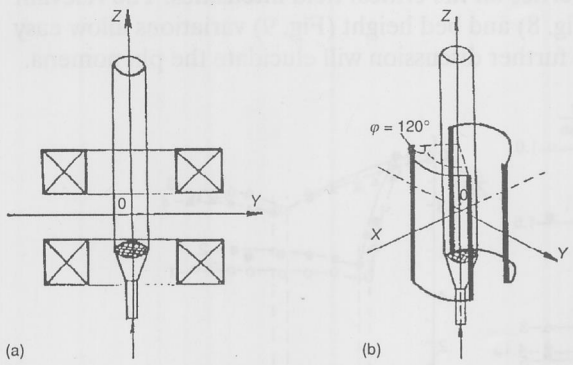

Figure 6. Experimental set-up (schematically for magnetization LAST studies in homogeneous fields [6]
a) Axial fields generated by Helmholtz pair; b) Transverse

In contrast to the studies commented above the results in [6] have been presented in accordance to the well-established approach used for phenomena description with Magnetization FIRST mode [2, 6–8]. Despite the field lines orientations the bed behaviour has common elements. The phase diagrams (Fig. 7) strongly indicate three bed states: ordinary bubbling bed, fluidization with bubbling and strings and a frozen bed. The detection of the critical field intensities has been made visually. These phase diagrams demon-

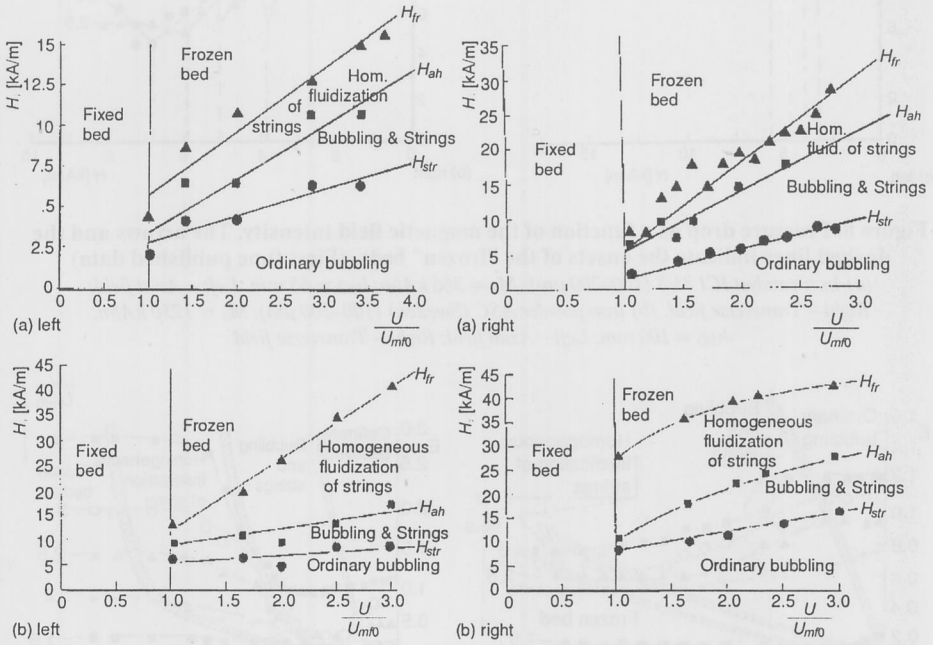

Figure 7. Phase diagrams. Effects of the field lines orientation and the magnetic properties of the particles represented by M_S;
(a) Air-Magnetite (315–400 mm, ρ_S = 5250 kg/m^3) h_{b0} = 100 mm; M_S = 478.5 kA/m. Adapted from [6]
Left – Axial field; Right – Transverse field;
(b) Air-Catalyst G3L (100–200 mm, ρ_S = 3000 kg/m^3) h_{b0} = 65 mm; M_S = 50.3 kA/m;
Left – Axial field; Right – Transverse field (First time published data)

strate the effect of the magnetic properties on the critical field intensities. The relevant data concerning the pressure drop (Fig. 8) and bed height (Fig. 9) variations allow easy detection of those critical points. The further discussion will elucidate the phenomena.

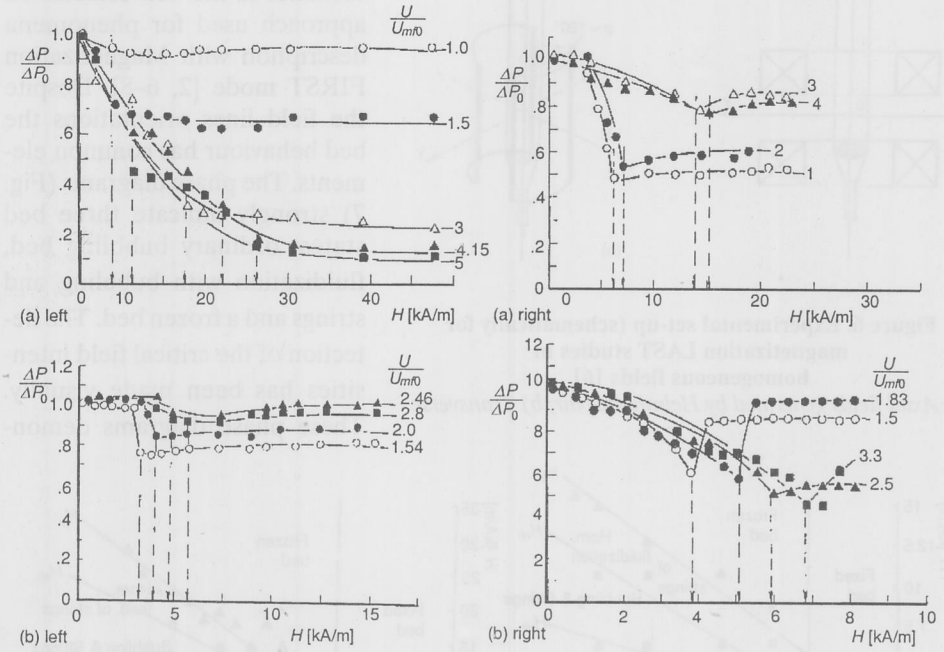

Figure 8. Pressure drop as a function of the magnetic field intensity. The arrows and the dashed lines indicate the onsets of the "frozen" beds. (First time published data)
(a) Iron catalyst ICI 35/8 (100–200 μm). M_S = 366 kA/m; h_{b0} = 65 mm. Left – Axial field; Right – Transverse field. (b) Iron powder ASC (Sweden) (100–200 μm). M_S = 1750 kA/m; h_{b0} = 100 mm. Left – Axial field; Right – Transverse field

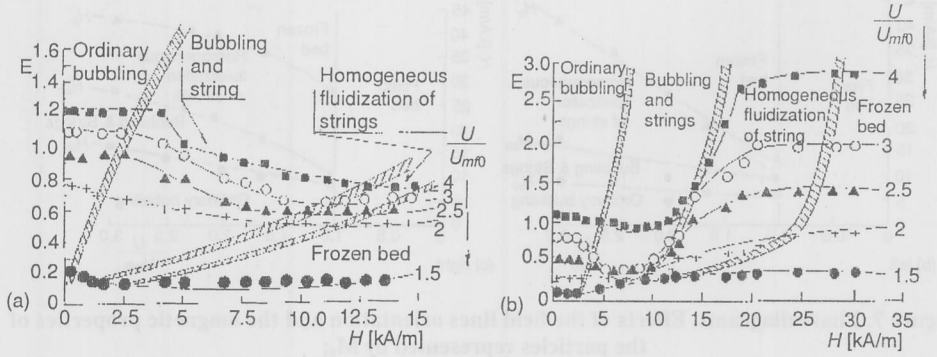

Figure 9. Relative bed height v/s the magnetic field intensity. Adapted from [6]. Air-Iron catalyst ICI 35/8 (BASF) (100–200 μm). M_S = 366 kA/m; h_{b0} = 65 mm.
(a) Axial field; (b) Transverse field

The data plotted indicate that the field intensity required to create a certain regime in a transverse field is approximately twice greater than those applied by an axial magnetic field. The explanation given in [6] will be commented further. The field effect orientation strongly affects the behaviour of the pressure drop curves and those of the relative bed height defined as

$$E = \frac{h - h_{b0}}{h_{b0}} \tag{2}$$

A principal condition for all experiments has been defined in [6] in order to obtain correct results:

- The maximum bed depth (in fixed and fluidized states) has been smaller than the height of the homogeneous field zone created in each of the magnetic systems used.

Under both fields applied and for low field intensities only a reduction of particle motion has been observed with a constant pressure drop across the bed. The field applied has no effect on the bubbling in the bed. At higher intensities short particle strings emerged (at the intensity H_{str}). The string length grew with the increase of field intensity. This phenomenon strongly affects the bubble evolution accompanied by suppressed bubbling. In an axial field the bubbles tend to elongate along the gas flow direction that seems like a suppression of bubbling. In a transverse filed the orientation of the strings in direction transverse to the gas flow changed the shape of the gas bubbles. The bubble shape altered from the classical pseudospherical from to elongated gas voids with long axis parallel to the field lines. Similar gas voids were observed in similar conditions but for the other mode of operation (Magnetization FIRST) [17] and commented in the first part of the series [8]. The bubbles will be commented further in this paper (see 4. BUBBLES).

At field intensity $H = H_{ah}$, the "homogeneous fluidization of the strings" started. A continuous decrease of string movement was observed up to the point at which bed "froze" (at the intensity H_{fr}) inspite the field orientation applied. In both fields the pressure drop decreases down to the freezing point. However, the bed depth curves have different behaviour. The reason of that is the strong "string-string" interaction that arranges the particles in the bed (see below). The frozen bed has been considered for a long time as a possibility to create a "magnetically stabilized bed" (under the action of axial fields) [2, 19, 20, 23, 24]. The main attraction is that the stronger field intensities suppress the bubbling and immobilize the particles. However, the particle-particle and string-string interactions strongly depend on the field orientation and the particle material properties. Moreover, the frozen bed differs significantly from that stabilized bed available with magnetization FIRST mode. Because of that the phenomenon will be commented in a separate point.

Frozen bed

Effect of the field orientation

The frozen bed has a fixed structure of particle strings. The structure is strongly anisotropic due the field orientation effect. In an axial field the pressure drop and the

bed depth are independent of a further increase of the gas velocity. In a transverse field the behaviour is just the opposite, because at the transitional point ($H = H_{fr}$) the pressure drop curves reached their minima. The further increase of the field intensity ($H > H_{fr}$) does not affect the bed depth in an axial field while in a transverse field the bed depth and the pressure drop increase after that minimum freezing point.

The mechanism of string-string interaction (see inset of Fig. 10) can explain the differences between bed heights in the regime of a frozen bed. The strings have forms of ellipsoids of revolution [21, 22] extended along the field lines (Fig. 10) and represent short induced bar magnets with repulsive forces between them (attractive forces exist between N and S poles, while between N-N and S-S poles the forces are repulsive). In an axial field the repulsive forces and the drag forces are perpendicular, so the bed height is limited by the maximum string length, and does not depend on the string arrangement in the bed. In a transverse field the repulsive forces and the fluid flow (*i. e.* the drag forces) are parallel. Hence, the both actions tend to increase the distance between the strings and the bed height as a whole.

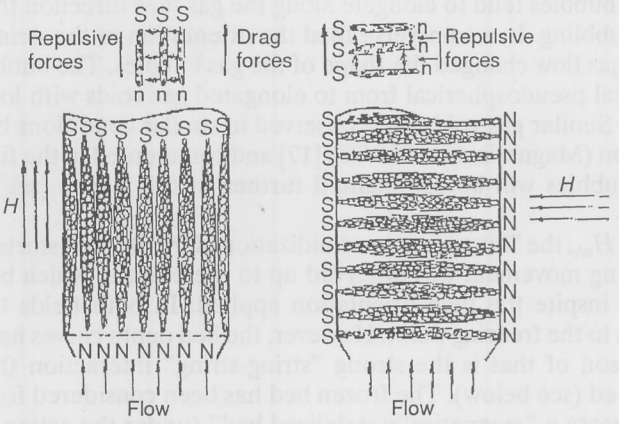

Figure 10. Schematic presentation of particle "strings" arrangement in a "frozen bed", Adapted from [6]; Left – Axial field, Right – Transverse field; Insets: String-string interaction and the orientation of the drag forces and the magnetic repulsive forces

The pressure drop data and the observations show that the point corresponding to the intensity H_{fr} corresponds to the point at which the pressure drop-field intensity curves reach their minima (Fig. 8). Figure 11 shows the H_{fr} values as a function of gas velocity. Despite the field orientation the field intensity, H_{fr}, required to "freeze" the fluidized particles is in proportion to the gas velocity. However, the field orientation affects the values of H_{fr} that can be attributed to the different string orientation with respect to the gas flow. A mechanistic model has been proposed in [6]. It explains the field orientation effect on H_{fr}. In an axial field the strings are streamlined along their long axis and the drag forces are minimal. In a transverse field the magnetic moments of rotation tend to orient the aggregates transversally to the fluid flow. It is clear that in a transverse field greater field intensities are required to achieve immobility of the fluidized strings, *i.e.* the bed freezing.

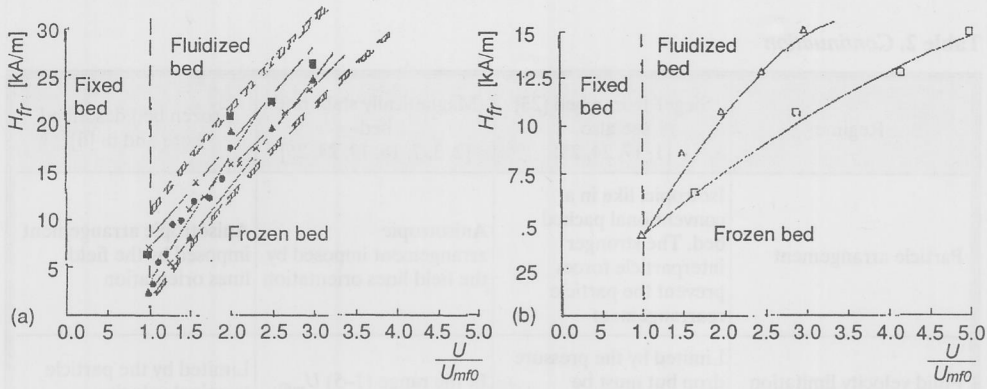

Figure 11. Freezing field intensities as a function of the gas velocity. Catalyst "H. Topsoe" h_{b0} = 100 mm. Effect of field lines orientation. Adapted from [6].

(a) Axial field: d_p, mm ■ – (100–200); ▲ – (200–315); × – (500–615); ● – (800–1000)

(b) Transverse field: d_p, μm □ – (100–200); △ – (200–315);

The frozen bed is a fixed bed with an induced stability like the "magnetically stabilized bed". In both cases the particle interactions stabilize the bed against the destructive action of the fluid flow. In some studies the term "condensed bed" has been introduced [22]. Comparative studies of the terms used are available in [6]. The term "frozen bed" used here differs from that used by Siegel [23]. Siegel's "frozen" beds can be created in the "Magnetization FIRST" mode and axial fields at higher field intensities [1, 17, 24, 25]. Fluidization is than impossible and the bed is like a piston. Table 2 compares the properties of the frozen beds obtained by different approaches and those of the magnetically stabilized beds (MSB).

Table 2. Particle beds with stronger interparticle magnetic forces: Frozen beds and magnetically stabilized beds. Different approaches give different results

Regime	Siegel' frozen bed [23] see also [1, 17, 24, 25]	Magnetically stabilized bed [2, 3, 7, 18, 19, 24, 25]	Frozen bed described here and in [6]
Operating mode and field applied	Magnetization FIRST in an axial field	Magnetization FIRST in both axial and transverse magnetic fields	Magnetization LAST in both axial and transverse magnetic fields
Pressure drop	Moderate to high	Axial field: • Low. Determined by the bed weight per unit cross section area of the column • Transverse field: Increases as the field intensity increases	Low in an axial field Moderate in a transverse field

Table 2. *Continuation*

Regime	Siegel' frozen bed [23] see also [1, 17, 24, 25]	Magnetically stabilized bed [2, 3, 7, 18, 19, 24, 25]	Frozen bed described here and in [6]
Particle arrangement	Isotropic, like in a conventional packed bed. The stronger interparticle forces prevent the particle rearrangement	Anisotropic arrangement imposed by the field lines orientation	Anisotropic arrangement imposed by the field lines orientation
Fluid velocity limitation	Limited by the pressure drop but must be retained in vessel	In the range (1–5) U_{mf0}	Limited by the particle terminal velocity
Bed fluidity	None	Moderate	None
Fluid solid contacting efficiency	High		High, but detailed investigations in a transverse field are not available yet
Performance as a filter for particulates		High. Depends on the field lines orientation and the particle arrangement with respect the gas flow	Data are not available yet

Effect of particle material properties on the freezing point

Obviously the field interaction with particles having high magnetic susceptibility needs field intensities lower than in the case of materials with low magnetic properties. This fact has been proved with Magnetization FIRST mode [17] (see Figs. 12 and 13 in [17]). Figures 12a,b show the particle property effect on the minimum freezing field intensity. Both figures demonstrate similar behaviours despite the different field lines orientations. The plots indicate that in an axial field the intensity needed for bed immobilization is approximately twice lower than that in a transverse field.

Minimum H_{fr} required

It is clear that the minimum field intensity required to freeze the particles depends simultaneously on the particle properties (M_s), the field orientations and the gas velocity excess above the minimum fluidization point (in absence of field). It was proved that the minimum field intensity required for bed stabilization with Magnetization FIRST mode could be determined graphically [7, 15]. The same approach may be applied here in the case of Magnetization LAST mode. The main idea is to approximate the points of H_{fr} obtained at higher field intensity and higher gas velocities by a smooth line. The

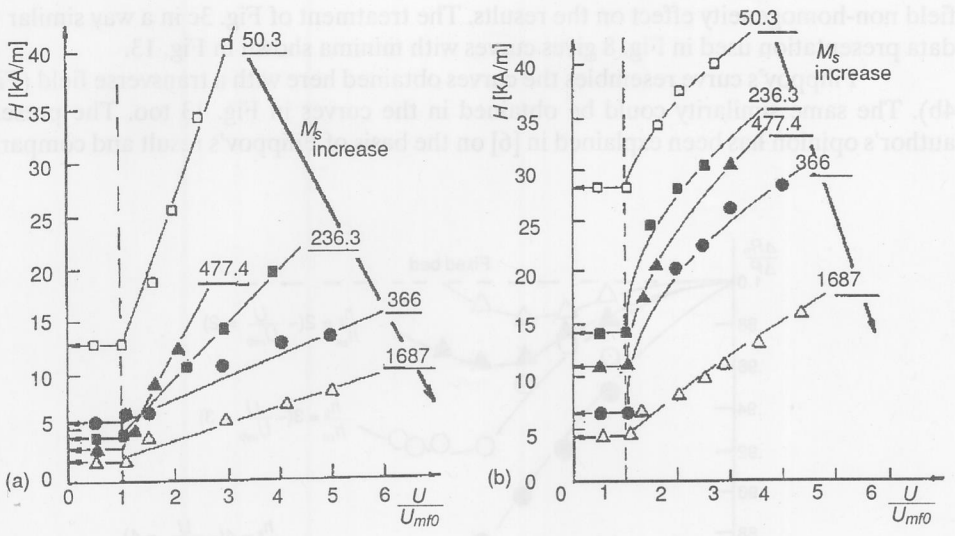

Figure 12. Freezing field intensities. Effect of the particle magnetic properties represented by the magnetization at saturation, M_s (the values at the ends of the solid lines). The arrows toward the vertical axis H, show the minimum field intensity required for bed freezing. For all situations, h_{b0} = 100 mm; d_p = 100–200 μm. (First time published data).
(a) Axial field; (b) Transverse field

detection of these field intensities is easier rather than those at lower gas velocities. After that the lines should be used to extrapolate the points toward the lower gas velocities. The intersection with a vertical line U/U_{mf0} = const (for example U/U_{mf0} = 1 separating the fixed bed and the frozen bed; see Figs. 7 and 12) defines the minimum value of H_{fr}. The same approach may be applied if the ratio $U/U_{mf0}>1$ is chosen at a desired bed expansion. The method is an alternative to the graphical determination from the pressure drop curves (Fig. 8). The pressure drop curves may be employed when the column wall is not transparent.

Experiments in non-homogeneous fields (field non-homogeneity effects on the results)

The experimental data for the pressure drop in an axial field obtained in [6] and these presented here do not confirm the Filippov's result [10, 11] shown in Fig. 2 because there are not sharply defined minima. The pressure drop curves are similar slightly to the results of Bologa and Syutkin [13] and confirm the data of Zrunchev and Popova [14, 15]. On the other hand the results of Doichev *et al.* [12] (Fig. 3c) obtained in a strongly non-homogeneous field with an axial symmetry give an additional information about the

field non-homogeneity effect on the results. The treatment of Fig. 3c in a way similar to data presentation used in Fig. 8 gives curves with minima shown in Fig. 13.

Filippov's curve resembles the curves obtained here with a transverse field (Fig. 4b). The same similarity could be obtained in the curves in Fig. 13 too. The present author's opinion has been explained in [6] on the basis of Filippov's result and compara-

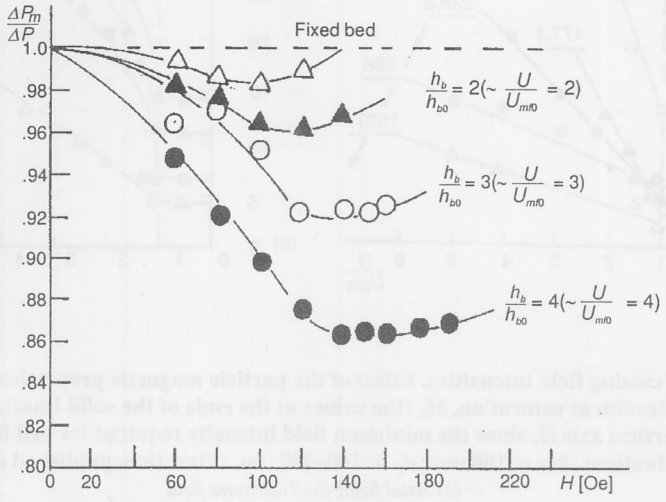

Figure 13. Pressure drops curve of Doichev *et al.* [12]. Data treatment by eq. (2) and presentation is in accordance with the plots in Fig. 8

tive experiments performed in the set-up shown in Fig. 14. However, for better elucidation of the experimental condition effect on the result it will be described briefly again. Filippov performed experiments with magnetite particles and 112–mm initial bed height in a 30 mm I. D. column (see Fig. 1). In the fluidized state the bed heights have been increased from 2 to 4 times as compared to the initial static height. The same range has been employed by Doichev *et al.* [12]. It is clear that, under these circumstances, the greater part of the bed is in a zone with strongly heterogeneous field (in axial and lateral directions). Moreover, at the top of the solenoid the field lines change their direction from parallel to normal with respect to the vertical axis.

The test performed in [6] with 130–mm initial static bed has simulated Filippov's experiments (see Fig. 14). The magnetic field was applied at a gas velocity from 2 to 4 times greater than U_{mf0}, so the bed heights were several times greater than the height of the magnetic system. The plots (Fig. 15) and the observances show that the minimum in the pressure drop curve appears at the point when the surface of the collapsing bed reaches the top of the magnetic system. At that point the field lines change their direction

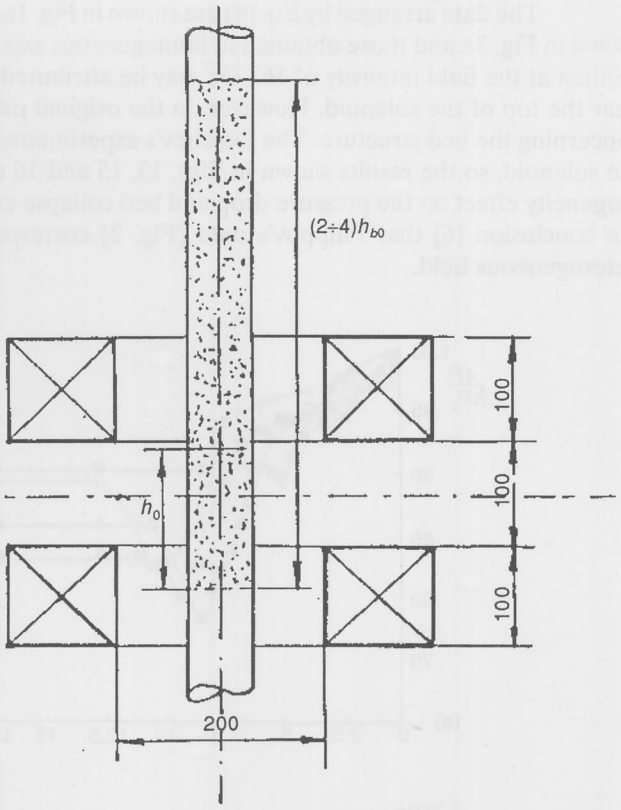

Figure 14. Experimental arrangement in test experiments performed in an axial magnetic field. Adapted from [6]. Dimensions in millimeters

from axial to normal as mentioned above. Hence, the shape of the pressure drop curves is similar to the shape of the curves obtained in a transverse field (Fig. 8). On the other hand the bed collapse curves are similar to those obtained in an axial field (Fig. 9).

The data plotted in Fig. 3b were treated in accordance with the common data presentation accepted in [6] and in the present paper. The equation (1) may be rewritten as

$$R = \frac{\left(\frac{h}{h_{b0}}\right) - \left(\frac{h}{h_{b0}}\right)_M}{\frac{h}{h_{b0}}} = 1 - \frac{E+1}{E_0+1} \tag{3}$$

where $E_0 = 1 - \frac{h_b}{h_{b0}}$ according to eq (2).

The treatment gives

$$E = (1-R)(E_0 + 1) - 1 \tag{4}$$

The data arranged by Eq. (4) are shown in Fig. 16. The plots resemble the curves shown in Fig. 3a and those obtained in homogeneous axial fields (see Figs. 9). The weak minima at the field intensity of 162 Oe may be attributed to the field non-homogeneity near the top of the solenoid. However, in the original paper there are no observations concerning the bed structure. The Doichev's experiments are performed at "the top" of the solenoid, so the results shown in Figs. 13, 15 and 16 demonstrate the field non-homogeneity effect on the pressure drop and bed collapse curves. Moreover, they confirm the conclusion [6] that Filippov's data (Fig. 2) correspond to the case of a strongly heterogeneous field.

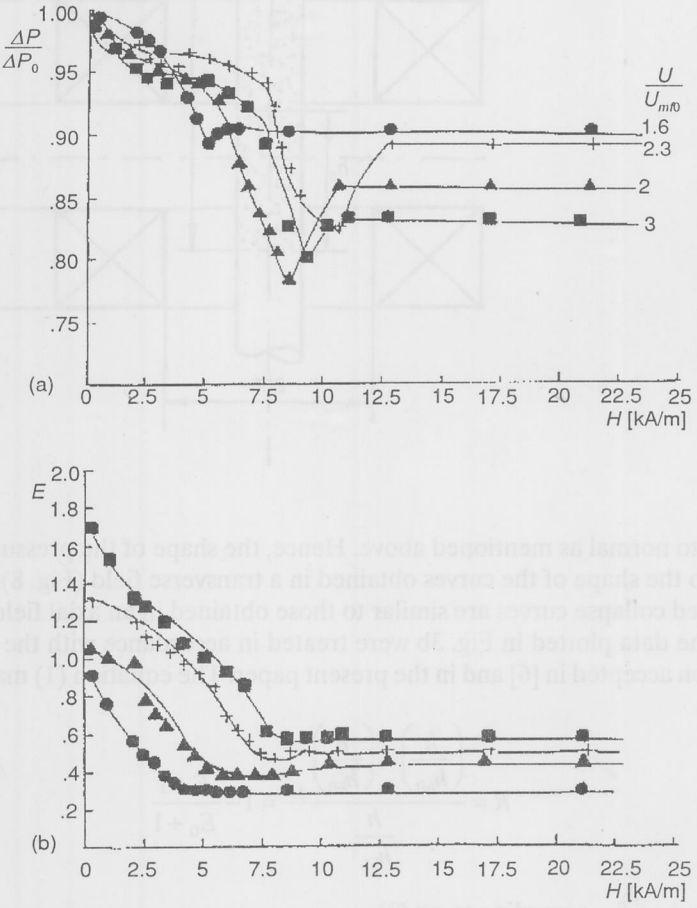

Figure 15. Experimental results obtained from the comparative experiments in an axial field. Adapted from [6]. Air Magnetite (315–400 μm). Dc = 65 mm; h_{b0} = 130 mm. *(a) Pressure drop. The arrows indicate the onsets of the "frozen" beds; (b) Relative bed height E*

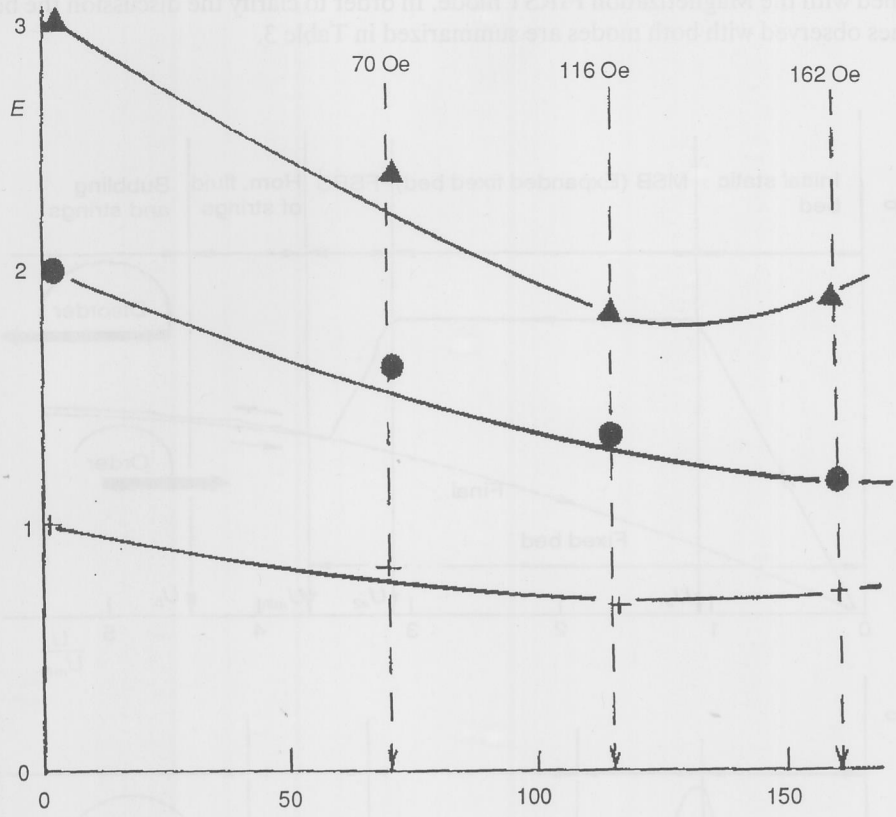

Figure 16. Doichev's results treated by eqs. (3–4)

AN ATTEMPT FOR GENERALIZED BED BEHAVIOUR DESCRIPTION

In contrast to Magnetization FIRST mode commented in [8] the data interpretation concerning the Magnetization LAST" mode did not pass through conflicting discussions. This may be explained by the little investigations performed and the fact that the phenomena do not allow interpretations contradicting the classic fluidization theory [26, 27]. The phenomena occurring with both modes of operation (magnetization modes) need generalization and estimation of common properties.

The results obtained in homogeneous magnetic fields (axial and transverse) have been discussed in [6] from the point of view of an order-disorder approach (ODT) based on a generalized thermodynamic approach of the description of disordered systems [28, 29]. The basis of that analysis is the fact that the sequences of states as well as the shape of the pressure drop curves in both magnetization modes give a possibility of

drawing a parallel between the bed behaviours. Figure 17 shows pressure drop curves obtained with the Magnetization FIRST mode. In order to clarify the discussion the bed regimes observed with both modes are summarized in Table 3.

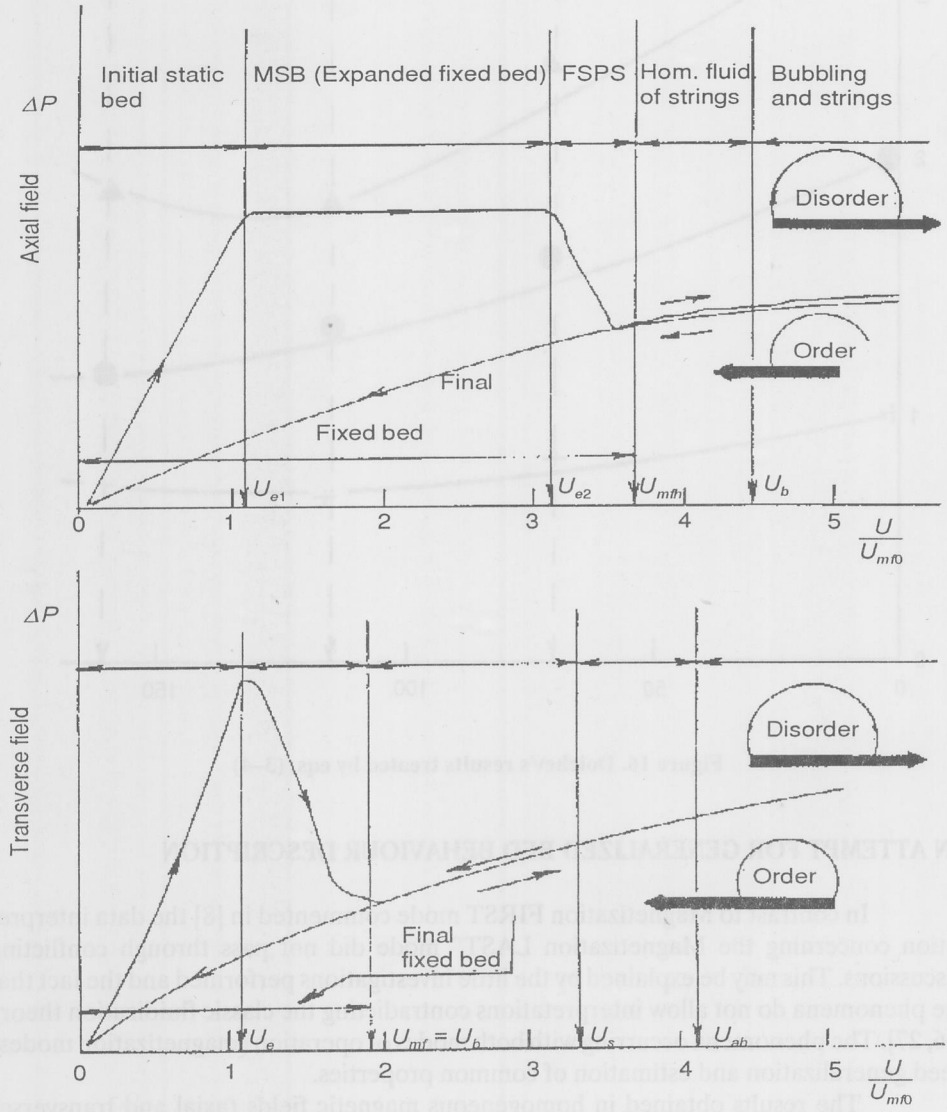

Figure 17. Typical pressure drop – gas velocity curves with separate sectors corresponding to different bed regimes in the mode" Magnetization FIRST". Adapted from [6]. Schematic presentation (no data points). Catalyst ICI 35/8 (100–200 μm); Dc = 65 mm; h_{b0} = 100 mm; H = 8 kA/m

Table 3. Regimes obtained with both magnetization modes and their macroscopic parameters

Term	Definition	Magnetization FIRST		Magnetization LAST	
		Axial field	Transverse field	Axial field	Transverse field
		Macroscopic parameters	Macroscopic parameters	Macroscopic parameters	Macroscopic parameters
Initial static bed	Classical fixed bed obtained after the filling of the material in the column	• The initial state for the fluidization. The field is applied on this bed. • The height, h, is constant. • The pressure drop ΔP is proportional to U	• The initial state for the fluidization. The field is applied on this bed. • The height, h, is constant. • The pressure drop ΔP is proportional to U	• The initial state of the bed before the fluidization	• The initial state of the bed before the fluidization
Magnetically stabilized bed	Expanded fixed bed at gas velocities above the minimum fluidization point in absence of a field. A transition state between the fixed bed and the fluidization	• ΔP = const. • The bed expands significantly	• ΔP decreases, but the onset of MSB requires pressure drops higher that those in an axial field • The bed expands significantly	• Does not exist with that operating mode	• Does not exist with that operating mode
Fixed structure of particle strings (FSPS)	A fixed bed between MSB and the fluidization onset. It occurs at the velocity U_{e2} (Rosensweig's U_T)	• The regime exists only under axial field orientation	• Does not exist under the action of transverse field	• Does not exist with that operating mode	• Does not exist with that operating mode
Homogeneous fluidization of particle strings	A fluidized bed of particle aggregates ("strings"). Oriented motions of the strings	• ΔP = const. • The bed height remains like that in MSB	• ΔP = const. • The bed height increases significantly	• ΔP decreases down to the "freezing" point • The bed collapses and its height decreases monotonically with the field intensity	• ΔP decreases down to the "freezing" point. An increase after that

Table 3. *Continuation*

Term	Definition	Magnetization FIRST		Magnetization LAST	
		Axial field	Transverse field	Axial field	Transverse field
		Macroscopic parameters	Macroscopic parameters	Macroscopic parameters	Macroscopic parameters
Fluidization with bubbling and strings	A fluidized bed of particle aggregates and bubbling	• ΔP pulses • The bed height remains constant	• ΔP increases slowly with U • The bed height remains constant	• ΔP decreases with H	• ΔP decreases with H
Ordinary bubbling regime	A classical fluidized bed	• Weak field effects • ΔP = const. • The bed height increases with U	• Weak field effects • ΔP = const. • The bed height increases with U	• The initial bed state before the field application	• The initial bed state before the field application
Final fixed bed	A fixed bed of strings. The structure depends on the field orientation	• Does not exist with that operating mode	• Does not exist with that operating mode	• ΔP = const. It does not depend on H, but is affected by U	• ΔP = const. It does not depend on H, but is affected by U
Frozen bed	A fixed bed of strings. The structure depends on the field orientation				

The fluidized system is affected by the concurrent actions of two physical fields: the first causing a disorder (fluid flow) and the second (magnetic field) causing order. Following this ODT analogy, the final bed regime corresponding to the increasing gas flow (see the label "Disorder" in Fig.17) corresponds to the point where the disordering action of the gas flow predominates over the ordering action of the field. With the decrease of gas flow rate ("Magnetization FIRST" mode) or with the increase of the field intensity ("Magnetization LAST" mode) starting from the regime of developed fluidization (a fully disordered system), the gas-particle system aspires to an ordered state due to the predominating action of the magnetic field. In both modes, the particle mobility decreases and the final state is a fixed bed having anisotropic structure. This allows the creation of symmetry diagrams (Fig. 18a,b) showing the formal symmetry of the regimes obtained with the Magnetization LAST mode and these occurring along the decreasing gas flow pressure drop curve of Magnetization FIRST mode. The same approach may be applied to the phenomena occurring parallel the increasing gas flow and these corresponding to Magnetization LAST mode (Fig. 19a,b).

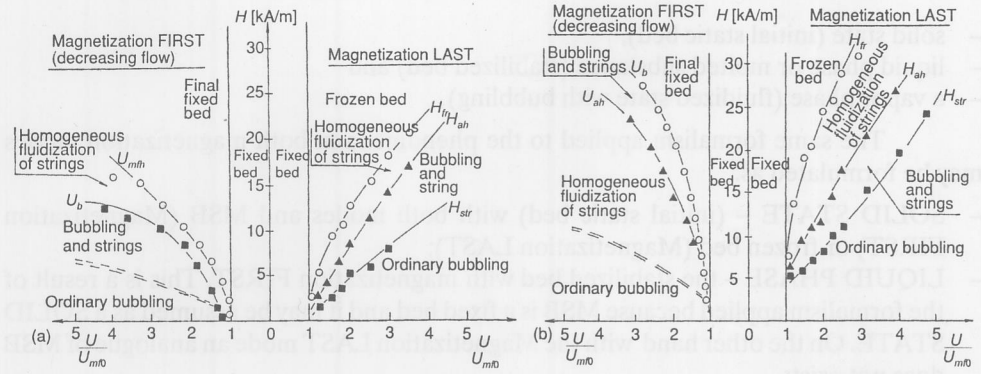

Figure 18. State diagrams showing the similarity between the Magnetization FIRST (decreasing flow) and the Magnetization LAST. Air-Magnetite (200–300 μm). Dc = 65 mm; h_{b0} = 100 mm

(a) Axial field; (b) Transverse field

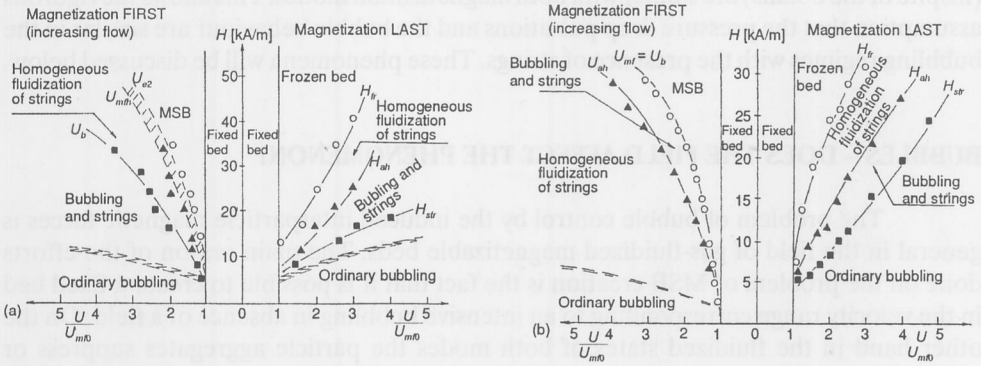

Figure 19. State diagrams showing the similarity between the Magnetization FIRST (increasing flow) and the Magnetization LAST

(a) Axial field. Catalyst G3L (100–200 μm). Dc = 65 mm; h_{b0} = 10;
(b) Transverse field: Air-Magnetite (200–315 μm). Dc = 65 mm; h_{b0} = 100

The presentation of the bed regimes by phase diagrams is a pseudo-thermodynamic approach conceived by Rosensweig [24, 30] to explain the phase diagrams in the "Magnetization FIRST" mode. Rosensweig's analogy concerns the velocity as an analog of pressure. According to Rosensweig (see Fig. 2 in [30]) the phase diagrams with the "Magnetization FIRST" mode resemble a thermodynamic phase diagram of a pure substance:

- solid state (initial static bed),
- liquid phase or molted substance (stabilized bed) and
- a vapor phase (fluidized state with bubbling).

The same formalism applied to the phenomena in both magnetization modes may be formulated as:

- SOLID STATE – (initial static bed) with both modes and MSB (Magnetization FIRST) or frozen bed (Magnetization LAST);
- LIQUID PHASE – the stabilized bed with magnetization FIRST. This is a result of the formalism applied because MSB is a fixed bed and it may be assumed as a SOLID STATE. On the other hand with the Magnetization LAST mode an analogue of MSB does not exist;
- VAPOR PHASE – the fluidized regimes: bubbling with strings or homogeneous fluidization of strings.

Despite the formal symmetry presented in Figs. 18 and 19 some asymmetries with respect the particular states exist due the hysteresis behaviour of fluidized system [31–33]. They will not be commented here. However, in order to support the further discussion it should note that bed behaviour corresponding to the fluidized regimes (inspite of the details) are similar with both magnetization modes. This allows the rigorous assumption that the pressure drop pulsations and the bubble behaviour are similar in the bubbling regimes with the presence of strings. These phenomena will be discussed below.

BUBBLES – DOES THE FIELD AFFECT THE PHENOMENON?

The problem of bubble control by the induced interparticle magnetic forces is general in the field of gas-fluidized magnetizable beds. The main reason of the efforts done on the problem of MSB creation is the fact that it is possible to create a fixed bed in the velocity range corresponding to an intensive bubbling in absence of a field. On the other hand in the fluidized states of both modes the particle aggregates suppress or develop the bubble evolution. Taking into account the symmetry drew in the previous part there is no practically differences between the fluidized states of "bubbling with strings" created with both magnetization modes.

Most of the investigations have been performed in axial magnetic field with Magnetization FIRST mode. The investigations in a transverse field [6–8, 13, 17, 18] are phenomenological and without quantitative results. Because of that the results obtained in axial field will be commented below.

Bologa and Syutkin [13] note that under a sudden turn on of the field it is possible to register the bubble formation near the incipient fluidization point in order to understand the physical reasons of the phenomenon. However, no quantitative data are available in [13]. These authors report that the bubbles shape follows the field lines orientation (axial and transverse have been used in [13]). Moreover, the bubble diameter does not follow the behaviour known in absence of a field (Bologa and Syutkin have referred to [34]).

Shumkov [35–37] has reported the first quantitative data on bubble behaviour in an air-fluidized bed of ammonia catalyst SA–1 (Russia). The experiments have been performed in a short solenoid (see the pictures in [17] and the comments in [8]). The transducer has been arranged as two microscopic electric lamps located vertically (19 mm distance) and two photo diodes. The distance between the source of the light (lamps) and the receptors (diodes) was 6 mm, so all the bubbles greater than 6 mm have been detected. The amplitudes of the electric signals have been recorded by an oscilograph.

Shumkov's results indicate that the bubble frequency varies in the range of 0.8 up to 5 Hz inspite the field intensity and the fluid flow rate. The most important fact obtained in these studies is the field effect on the vertical bubble dimension. The vertical bubble dimension, y, increases with the increase of the gas velocity, while increase of the field intensity has an opposite effect. Moreover, y decreases with increase of the distance h above the supporting grid. Figure 20 presents Shumkov's results [35, 36]. This strongly indicates that the anisotropy imposed by the by the axial field affects the bubble shape.

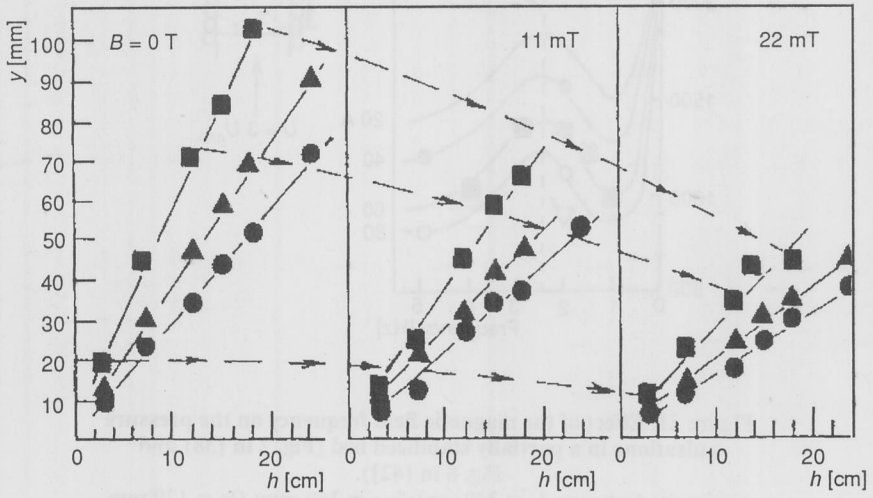

Figure 20. Shumkov's results [35, 36]. The simultaneous effect of the gas velocity and the magnetic field induction B, on the vertical bubble dimension y
Gas velocity effect: U, m/s, ■ – 0.9; ▲ – 0.85; ● – 0.645
Adapted from [35]. The present author adds the dashed lines and arrows in order to demonstrate the overall effect on y

Jovanović and co-workers [39–42] have done the second important contribution concerning the bubbling in a magnetizable gas-fluidized bed. Jovanović has accepted the term "partially stabilized fluidized bed" for the regime corresponding to bubbling with particle strings. The technique of bubble size measurements employed in these studies

use pressure signals from two pressure probes located vertically along the column axis. Two versions have been employed. The method developed by Zhang *et al.* [43] has been employed in [38, 42] while that developed by Sitnai [44, 45] has been used in [39, 41]. There is no information about the technique applied in [39], but this is insignificant because both methods are similar (see comments in [39]).

Jovanović *et al.* [38, 42] have detected that the natural bubble frequency (NBF) in a partially stabilized bed is in the range 1–5 Hz that confirm the results of Shumkov. Moreover, these authors have applied an external time varying field in order to obtain a resonance conditions for pressure fluctuations in the bed. The results are shown in Fig. 21. The plot indicates that the resonance occurs at a field frequency about 2 Hz that is close to NBF.

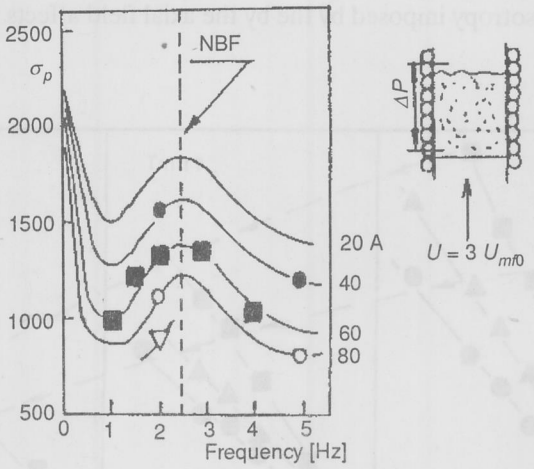

Figure 21. Effect of the magnetic field frequency on the pressure pulsations in a partially stabilized bed (Fig. 2 in [38] and Fig. 8 in [42]).
Air-ferrite (average d_p = 240 μm); h_{b0} = 160 mm; Dc = 120 mm. Adapted from [42]. The values on the right of the figure show the electric current strength through the solenoid (higher currents generate higher field intensities and *vice versa*). The present author adds the arrows in order to demonstrate the general ten-

The bubble size is strongly influenced by the gas velocity and the field intensity. Figures 22 a, b show that the bubble diameter d_b increases parallel to the gas velocity and decreases with the increase of the field intensity. The data plotted confirm the results of Shumkov [35–37] shown in Fig. 20. The column diameter in both studies are close (Shumkov – Dc = 140 mm; Jovanović – Dc = 120 mm). However, the similarity of the

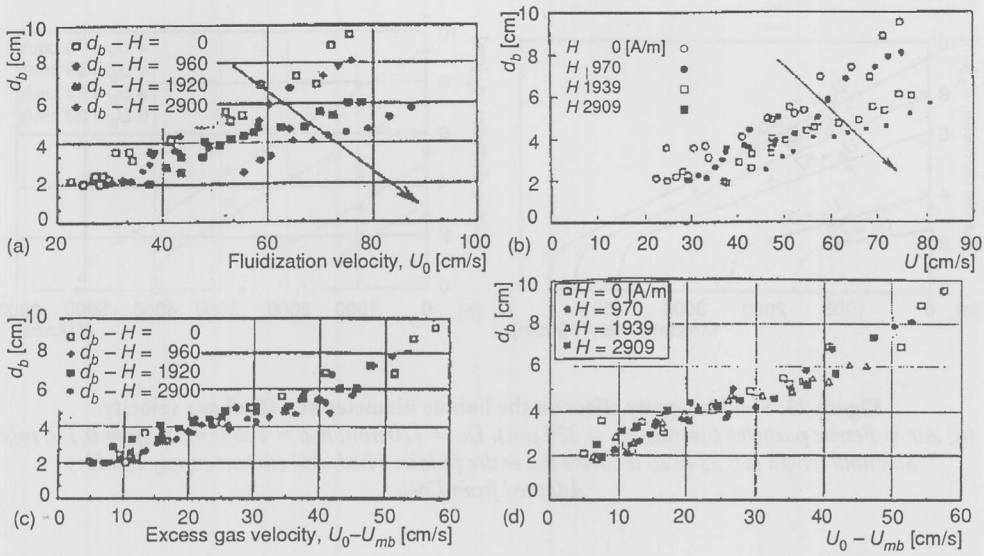

Figure 22. Bubble diameter as function of the gas velocity U_0. Effect of the field intensity
(a) Air =Ferrite particles (average d_p = 320 μm). Dc = 110 mm; h_{b0} = 100; U_{mf0} = 0.156 m/s Solenoid length is 0.33 m so it covers the entire fluidized bed. AC current supply (50 Hz). Adapted from [39]; (b) The conditions are like those in Fig. 22a, but h_{b0} = 90 mm; Adapted from [41];
(c) The conditions are like those in Fig.22a, but the d_b is presented a function of the excess gas velocity ($U_0 - U_{mb}$). Adapted from [39]; (d) The conditions like in Figs. 22a; h_{bo} = 90 mm. Adapted from [41]

results should be considered with caution due to the differences in the experimental techniques used. The technique applied by Shumkov detects the vertical dimension of an elongated bubble (along the field lines – see [8]), while the pressure signal techniques [43–45] assume the bubble shape as a "pseudo-sphere". The latter technique does not give qualitative information about the gas void deformation due to the magnetic inter-particle forces. Similar results are shown Fig. 22c, d when the bubble size variations are presented as a function of excess gas velocity (U_0–U_{mb}).

The field effect on the bubble diameter is shown in Figs. 23a,b. Both figures show that the bubble size decreases as the field intensity is increased. The opposite tendency exists when the bubble diameter is plotted (Fig. 24) against the difference ($H_{ms} - H$) or ($H_c - H$) termed "a magnetic field deficiency" [39, 41] that confirm the results of Shumkov.

The result of Jovanovic commented above give a very important information about the field effect on the gas void evolution. The works referred [38–42] do not interpret the results from the point of view that the field-induced anisotropy elongates the bubbles. However, only such phenomenon interpretation may explain the fact that the bubble diameter d_b (80–100 mm – see Figs. 21–24) approaches the column diameter

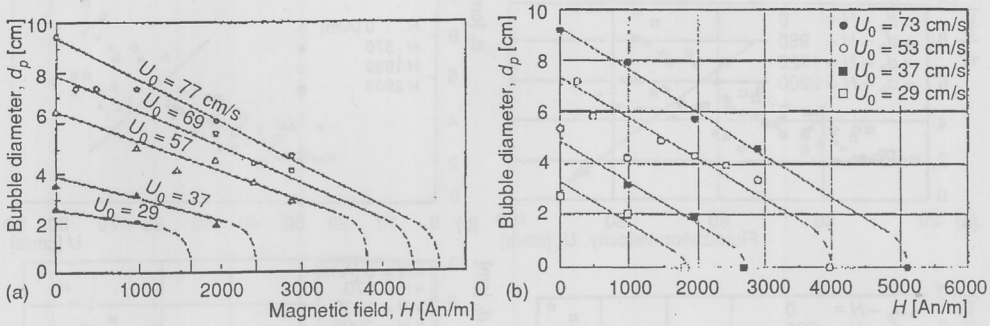

Figure 23. Field intensity effect on the bubble diameter at a fixed gas velocity.
(a) Air = Ferrite particles (average d_p = 320 μm). Dc = 110 mm; h_{b0} = 100 mm; U_{mf0} = 0.156 m/s Solenoid length is 0.33 m so it covers the entire fluidized bed. AC current supply (50 Hz). Adapted from [39];

of 110 mm. In a conventional gas-fluidized beds such dimensions of the bubbles indicate the onset of a slugging regime. However, in magnetizable beds under an axial field this regime does not exist (see Fig. 17 and the comments in [6]). The assumption of the bubbles as pseudo-spherical (the basis of the measuring technique applied) does not give adequate interpretations of the phenomena.

Despite the well-documented results these studies have not been developed toward a complete bubble shape description that may be attributed to the restrictions imposed by the measuring techniques used.

The bubble rise velocity U_{br} as function of the bubble diameter is shown in Fig. 25. The data are consistent with the results from non-magnetic fluidization [27]. The field intensity has no effect on the bubble rise. It was commented in [39] that when the bubble diameter becomes comparable to that of the vessel (d_b>8 cm) the bubble rise velocity

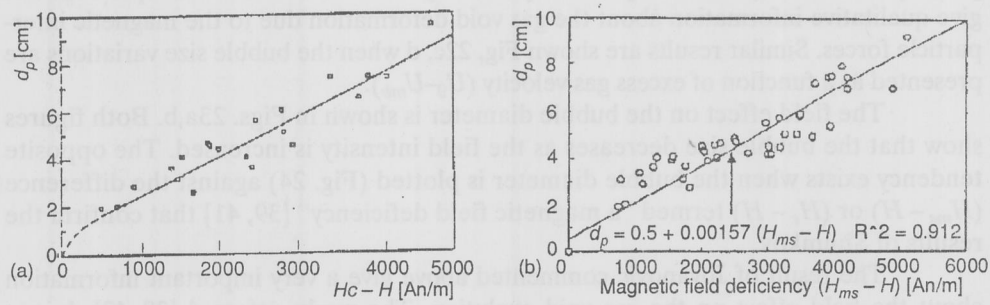

Figure 24. Bubble diameter v/s the magnetic field deficiency
(a) The conditions are like those in Fig. 23a. Adapted from [39];
(b) The conditions are like those in Fig. 23b. Adapted from [41]

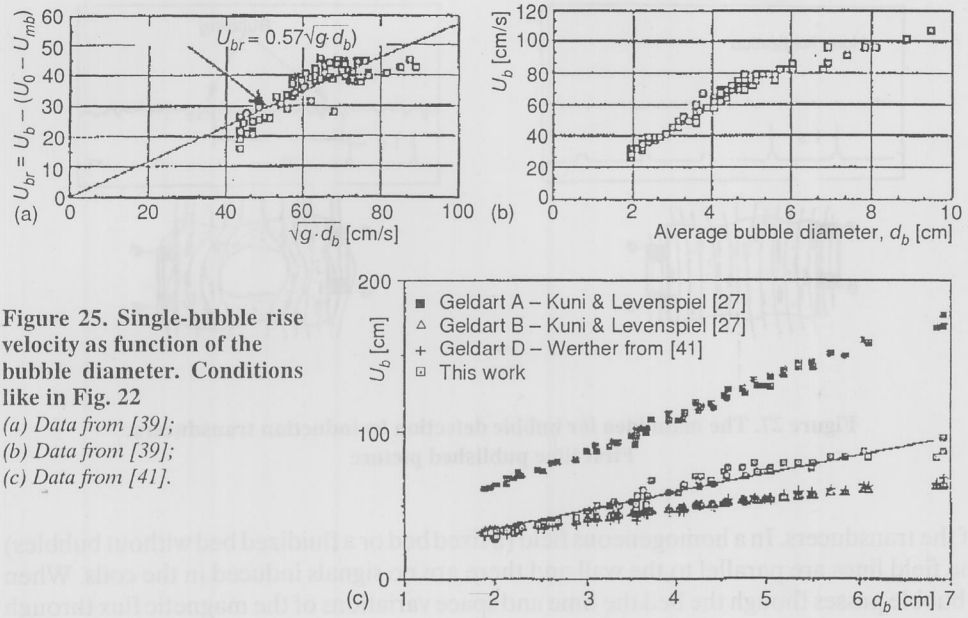

Figure 25. Single-bubble rise velocity as function of the bubble diameter. Conditions like in Fig. 22
(a) Data from [39];
(b) Data from [39];
(c) Data from [41].

becomes independent of its diameter and approaches the slug rise velocity. However, slugging has not been observed in these studies as mentioned above.

The present author has detected the bubble frequency by induction transducers placed at the column wall (Fig. 26) The techniques is still in progress, but short comments are available in [16, 17]. The bubble motion disturbs the field lines crossing the short coils

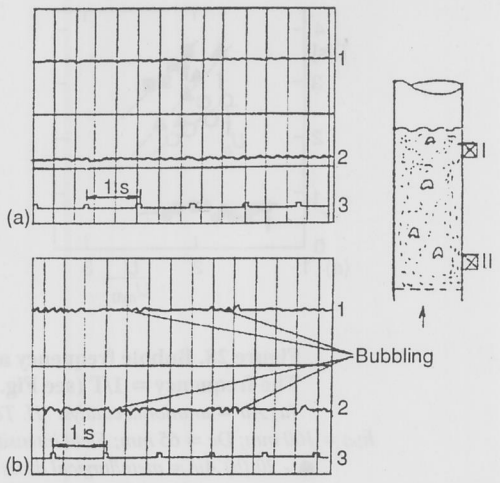

Figure 26. Bubble detection and regime identification by induction transducers in an axial field. Inset, the position of two transducers at the wall
I – top transducer;
II – bottom transducer;
(a) Records of the signal in a homogeneous fluidization of string [16, 17];
(b) Records of the signal generated by the bubbles [16, 17]

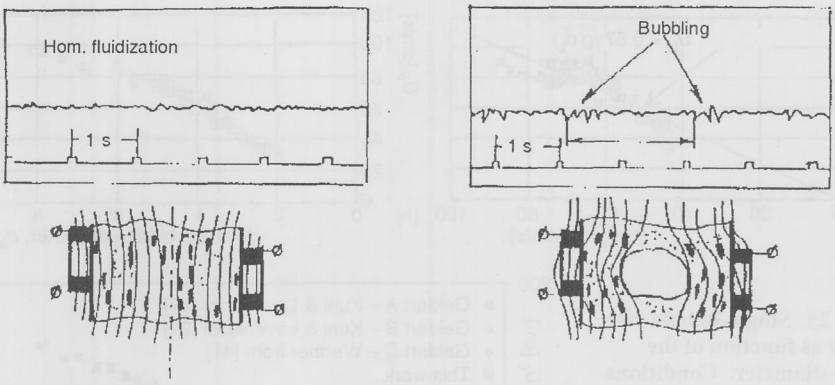

Figure 27. The main idea for bubble detection by induction transducers. First time published picture

of the transducers. In a homogeneous field (a fixed bed or a fluidized bed without bubbles) the field lines are parallel to the wall and there are no signals induced in the coils. When a bubble passes though the bed the time and space variations of the magnetic flux through the coils generate an electric signal [21] (Fig. 27). This phenomenon is basic and absolutely detects the motion of the ferromagnetic solids. Figure 28 presents the decrease of the bubble frequency with the increase of the field intensity and the opposite effect of the gas velocity above the minimum bubbling point. The plots indicate that the bubble frequency varies from 0.3 Hz to 1 Hz that is consistent with the data of Jovanović [38, 42] (f = 2 Hz shown in Fig. 21) and Shumkov [36].

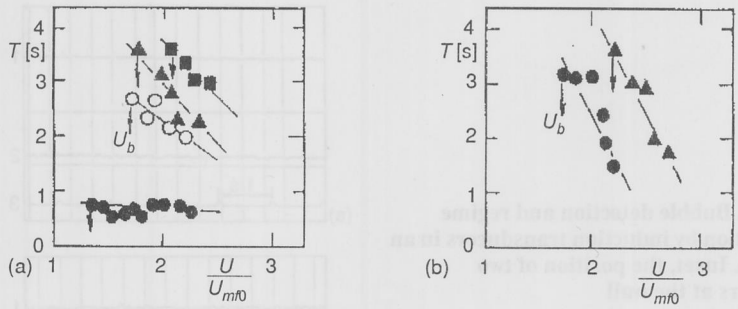

Figure 28. Bubble frequency as a function of the gas velocity. The frequency = 1/T (see Fig. 27). First time published data
(a) Air = ammonia catalyst "H. Topsoe" KM-1 (d_p = 800–1000 μm); h_{b0} = 100 mm; Dc = 65 mm; Field intensity effect, H, kA/m: ■ – 13; ▲ – 10.5; ○ – 4.3 ● – 20;(b) Air = metallurgical dross (d_p = 800–1000 μm); h_{b0} = 50 mm; Dc = 65 mm; Field: H, kA/m; ● – 4; ▲ – 16

CONCLUSIONS

The results discussed here concerns various problems of magnetization FIRST mode of gas-fluidized magnetizable beds of Geldart's B particles. The data commented cover the development of the studies with that magnetization technique over 40 years since the first reports of Filippov till 1998. The comparative analysis and experiments designed allow easy detection of the effects of the experimental conditions on the experimental results.

The "Magnetization LAST" mode offers a possibility to control the solid phase movement and the bubble shapes. The efficiency of regimes commented with both magnetization modes need detailed investigation on the mass and heat transfer operations (see the next Part 3 of the series) in gas fluidized magnetizable beds that is wide area for investigations.

NOMENCLATURE

B [T] – magnetic field induction
Dc [m] – column diameter
d_b [cm] – bubble diameter (a symbol used by Jovanović and co-workers)
d_p – particle diameter
E – relative bed height, $E = (h_b - h_{b0})/h_{b0}$
g [m^2/s] – gravitational constant
H [A/m] – magnetic field intensity
Hc [A/m] – minimum field intensity requred for bed stabilization (defined in [39] as critical field intensity)
H_{ms} – corresponds to Hc, but the symbol is used in [41]
H_{str} [A/m] – magnetic field intensity at which particle "strings" emerged
H_{fr} [A/m] – freezing field intensity
h [cm] – a distance between the grid and the transducer in Shumkov's experiments (Fig. 20)
h_b [m] – bed height
h_{b0} [m] – initial bed height
M_s [A/m] – magnetization at saturation
ΔP [Pa] – pressure drop
ΔP_0 [A/m] – pressure drop at zero field intensity
U [m/s] – superficial gas velocity
U_0 [cm/s] – fluidization velocity (Jovanović's data in Fig. 22. It corresponds to U used here)
U_{mb} [cm/s] – minimum bubbling velocity (Jovanović's data in Fig. 22. It corresponds to U_b used here)
U_{mf0} [m/s] – minimum fluidization velocity in the absence of a magnetic field
U_{mfh} [m/s] – velocity at the onset of a "homogeneous fluidization of strings" (see Fig. 10)
U_{e1} [m/s] – velocity at onset of MSB (axial field, Magnetization FIRST)
U_{e2} [m/s] – velocity at the break-down of MSB (axial field, Magnetization FIRST)
U_b [m/s] – bubbling velocity (see Fig. 10, Magnetization FIRST)
U_{br} [cm/s] – single-bubble rise velocity (the symbol U_b is used too in Figs. 25b,c)
y [mm] – vertical bubble dimension (Shumkov results – Fig. 20)

Greek letters

ρ_s – density of solids
σ_p – dispersion of the pressure pulsations, computer units (Fig. 21)
σ_s – density of solids

Abbreviations

MSB – magnetically stabilized bed
NBF – natural bubble frequency
FSPS – fixed structure of particle strings (see Fig. 17 and Table 3)

REFERENCES

[1] Kirko, I. M., Filippov, M.V., The Features of a Suspended Bed of Ferromagnetic Particles in a Magnetic Field, *Journal Techn. Fiziki, 30* (1960), pp. 1081–1084
[2] Rosensweig, R. E., Fluidization: Hydrodynamics Stabilization with a Magnetic Field, *Science, 204* (1979), pp. 57–60
[3] Casal, J., Contributio a l'estudi dels fenomens de transport en la fluiditzatio particulada, Doctoral Thesis, Univ. Politechnica de Catalunya,Barcelona, 1982
[4] Johnson, T. W., Melcher, J. R., Electromechanics of Electrofluidized Beds, *Ind. Eng. Chem. Fund., 14* (1975), pp. 146–153
[5] Dietz, P.W., Melcher, J. R., Interparticle Electrical Forces in Packed and Fluidized Beds, *Ind. Eng. Chem. Fund., 17* (1976), pp. 28–32
[6] Hristov, J. Y., Fluidization of Ferromagnetic Particles in a Magnetic Field. Part 2: Field Effects of Preliminarily Fluidized Beds, *Powder Technology, 97* (1998), pp. 35–44
[7] Hristov, J. Y., Fluidization of Ferromagnetic Particles in a Magnetic Field. Part 1: The Effect of the Field Lines Orientation on Bed Stability, *Powder Technology, 87* (1996), pp. 59–66
[8] Hristov, J. Y., Comments on Gas-Fluidized Magnetizable Beds in a Magnetic Field, Part 1: Magnetization FIRST Mode, *Thermal Science, 2* (1998), 2, pp. 3–25
[9] Geldart, D., Types of Gas Fluidization, *Powder Technology, 7* (1973), pp. 285–292
[10] Filippov, M.V., A Fluidized Bed of Ferromagnetic Particles and the Action of a Magnetic Field on It, *Troudii Inst. Fiziki Latv.* SSR, *12* (1961), pp. 215–236
[11] Filippov, M.V., Some Properties of a Suspended Bed of Ferromagnetic Particles in a Magnetic Field, *Voprosii magn. gidrodinamiki i dinamiki plasmii*, Riga, 1962, pp. 637–642
[12] Doichev, K., Petkov, J., Dimitrov, V., Fluidized Bed in an Electromagnetic Field, *Rudodobiv & Metallurgia* (Mining and Metallurgy), Bulgaria, *7* (1965), pp. 16–19
[13] Bologa, M. K., Syutkin, S. U. , Electromagnetic Field Effect on the Structure and the Hydrodynamics of a Fluidized Bed (in Russian), *Elektronna obrabotka materialov, 1* (1977), pp. 37–42
[14] Zrunchev, I., Popova, T., A Method for a Reduction of the Hydraulic Resistance of Ferromagnetic Catalysts and Materials (in Bulgarian), *Chemistry and Industry, 51* (1979), pp. 256–258
[15] Zrunchev, I., Popova, T., Bed Stabilization and Heterogeneous Processes in Gradient and Non-Gradient Magnetic Fields (in Bulgarian), *Ann. Reports of UCTM*, Sofia, *27* (1980), 4, pp. 181–188
[16] Hristov, J. Y., Gas-Fluidization of Ferromagnetic Granular Materials in an External Magnetic Field (in Bulgarian), PhD Thesis, UCTM, Sofia, 1994
[17] Penchev, I. P., Hristov, J. Y., Behaviour of Fluidized Beds of Ferromagnetic Particles in an Axial Magnetic Field, *Powder Technology, 61* (1990), pp. 103–118
[18] Penchev, I. P., Hristov, J. Y., Fluidization of Ferromagnetic Particles in a Transverse Magnetic Field, *Powder Technology, 62* (1990), pp. 1–11
[19] Rosensweig, R. E., Process for Operating a Magnetically Stabilized Fluidized Bed, U.S. Patent 4 125 927, Sept. 24, 1980
[20] Sonolikar, R. L., Magneto-Fluidized Beds, Transport in Fluidized Particle Systems (Ed. A. Mujumdar), Elsevier, New York, 1989, pp. 359–422
[21] Tamm, I. E., Fundamentals of Electricity (Osnovii teorii elektrichestva), Nauka publ., Moskow, 1966
[22] Zhu, Q., Li , H., Study on Magnetic Fluidization of Group C Powders, *Powder Technology, 86* (1996), pp. 179–185
[23] Siegel, J. H, Magnetically Frozen Beds, *Powder Technology, 55* (1988) p. 127
[24] Rosensweig, R. E., Siegel , J. H., Lee, W. K., Mikus, T., Magnetically Stabilized Fluidized Solids , *AIChE J., Symp. Ser. 77* (1981), 205, pp. 8–16

[25] Saxena, S. C., Shrivastava, S., Some Hydrodynamic Investigations of Magnetically Stabilized Air-Fluidized Bed of Ferromagnetic Particles, *Powder Technology, 64* (1991), pp. 57–67
[26] Davidson, J. F., Harrison, D., Fluidized Particles , University Press, Cambridge, 1963
[27] Kunii, D., Levenspiel, O., Fluidization Engineering, 2nd edn., Butterworth-Heinemann, Boston, 1991
[28] Ziman, J. M., Models of Disorder, Cambridge University Press, Cambridge,1979
[29] Careri, G., Ordine e disordine nella materia, Gius Laterza & Figli Spa., Roma/Bari, 1982
[30] Rosensweig, R. E., Process for Operating a Magnetically Stabilized Fluidized Bed, U.S. Patent 4 125 927, (1978)
[31] Arnaldos, J., Estudi de l'estabilitzacio dels llits fluidizacio solid-gas mitjancant l'aplicacio d'un camp magnetic (in Catalan), Doctoral Thesis, UPC, Barcelona, 1985
[32] Casal, J., Arnaldos, J., The Structure of Magnetized-Fluidized Beds, *Powder Technology, 64* (1991), pp. 43–48
[33] Zimmels, Y., Resnik, W., Harel, O., Hysteresis Phenomena in Magnetized-Fluidized Beds., *Powder Technology, 64* (1991), pp. 49–55
[34] Buyevich, Yu., On the Bubble Motion in a Fluidized Bed (in Russian), *Inz. Fiz. J., 28* (1975), 5, pp. 773–780
[35] Shumkov, St., Doctoral Thesis (in Bulgarian), UCTM, Sofia, 1973
[36] Shumkov, St., Ivanov, D., Gas Bubble Behaviour in a Fluidized Bed under an Electromagnetic Field (in Bulgarian), *Chemistry and Industry, 46* (1974), 3, pp. 108–110
[37] Shumkov, St. , Ivanov, D., Velev, K., Pressure Fluctuations in a Fluidized Bed under a Magnetic Field, *Ann. Reports of UCTM-Sofia, 32* (1975), 3, pp. 87–95
[38] Jovanović, N. G., Colakyan, P., Jovanić, P., Vuković, D.V., Performance of Magnetically Stabilized Fluidized Beds, 8th Congress CHISA 84, paper No . 767, Prague, Czech Republic, Sept. 3–7, 1984
[39] Jovanović, G. N., Jovanović, Z. R., Vinjak-Novaković, G., Vuković, D. V., Bubble Size in Magnetically Controlled Fluidized Beds, In: *Fluidization VI*, (1989), Eng. Foundation, N.Y., pp. 237–244
[40] Sajc, L. M., Jovanović, Z. R., Jovanović, G. N., Vinjak-Novaković, G., Kundaković, L., Obradović, B., Vuković, D.V., *J. Serb. Chem. Soc.,57* (1992), 5–6, pp. 297–307
[41] Jovanović, G. N., Jovanović, Z. R., A Novel Approach in Controlling Performance of Fluidized Beds: Bubble Size and Fluidization Regime in Magnetically Controlled Fluidized Beds, Symp. on Novel Reactor Techniques for Heterogeneous Systems., *AIChE Ann. Meeting*, 1993, Nov. 7–12, St. Luis, Paper No. 28i
[42] Jovanović, Z. R., Jovanović, G. N., Vinjak-Novaković, G., Effect of Magnetic Field on Bubble Behaviour in Partially Stabilized Gas-Ferromagnetic Particles Fluidized Beds., *Proceedings,* 2nd Yugoslavian Chemical and Process Engineering, May 11–15, 1987, Dubrovnik, *2,* pp, 30–34
[43] Zhang, M. C., Walsh, P. M., Beer, J. M., Determination of Bubble Size Distributions from Pressure Fluctuations in a Fluidized Bed Combustor, 7th Int. Conf. on Fluidized Bed Combustion, Philadelphia, PA, Oct. 25–27, 1982
[44] Sitnai, O., Dent, D. C., Whitehead, A. B., Bubble Measurement in Gas-Solid Fluidized Beds, *Chem. Eng. Sci., 36* (1981), 9, p. 1583
[45] Sitnai, O., Determination of Bubble Parameters from Pressure Fluctuations in a Fluidized Bed, CHEMECA'83, 11th Australian Conf. on Chem. Eng., 1982, paper 16b, pp. 539–545

Author's address:

Jordan Y. Hristov
Department of Chemical Engineering
University of Chemical Technology and Metallurgy
1756 Sofia, 8 Kl. Ochridsky str., Bulgaria,
E-mail: jyh@uctm.edu

Paper submited: November 20, 1999
Paper revised: November 25, 1999
Paper accepted: March 3, 2000